Proceedings of the
Annual Stability Conference
Structural Stability Research Council
Charlotte, North Carolina, April 11-14, 2023

Progression of failure in cold-formed steel diaphragms sheathed with steel deck

Sheila Ariana[1], Hernan Castaneda[2], Kara D. Peterman[3]

Abstract
Light repetitively framed lateral systems are hallmarked by the high degree of redundancy in the structural system. This can manifest as complex load paths which can be difficult to distill into traditional limit state design. During a suite of recent cantilever diaphragm testing at the University of Massachusetts Amherst, load was observed to transmit from steel deck to side-lap fasteners, then to edge and support fasteners, and eventually forcing flexural torsion in the steel joists which buckled the clip angles (web of the joist-to-web of the ledger connection). Understanding this progression is critical to making informed design decisions. To confirm the experimental findings, a high-fidelity finite element model is created to match the experimental specimen geometry. The specimen is a 10'x15' diaphragm with cold-formed steel joists spaced at 2' on center. Joists frame into two ledgers as the collectors via clip angles, a standard detail in ledger-framed construction. The specimen is sheathed with steel deck. Fasteners are the connecting elements between ledgers and steel deck, joists and steel deck, and two steel decks. The diaphragm is designed to be fixed on one side, and to be loaded monotonically on the other side, representing a cold-formed steel framed floor subjected to lateral loading. The finite element model uses shell elements, and connections behavior and contacts are fully defined. The model is capable of capturing experimental progression of failure, up to and including buckling of the clip angles. With a fully-validated finite element model, it is possible to better understand load path for these repetitively framed systems, and the influence of design on the progression of failure.

1. Introduction and Motivation

In recent years, the usage of cold-formed floor systems as lightweight frames have been growing significantly in North America. These systems have been substituted for the wood framed floors which have been traditionally utilized as cost-effective systems (Zhang & Xu, 2018). A series of cold-formed steel joists, connected to the ledgers with an equal distance from one another and sheathed with subfloors, accounts for a cold-formed steel floor system. This system is usually capped with various sheathing panels including plywood, oriented strand board (OSB), cementitious board or corrugated steel deck (Zhang & Xu, 2018).

[1] PhD Student and Graduate Research Assistant, University of Massachusetts Amherst, <sariana@umass.edu>
[2] PhD, Project Consultant, Simpson Gumpertz & Heger (SGH), <hcastaneda@sgh.com>
[3] Associate Professor, University of Massachusetts Amherst, < kdpeterman@umass.edu >

Several experimental studies have been performed on cold-formed steel diaphragms to clarify the complicated load path and potential failure modes in these systems. Experimental modeling of the wood shear walls shows that the response of the connections under monotonic loading is highly non-linear (JD Dolan, 1992). The damage of the sheathing boards by fasteners is resulted from the movement between frame and sheathing panels, creating non-linear behavior (Hein Tun, 2014). Other experimental tests aiming to evaluate monotonic and cyclic responses of the cold-formed steel-framed diaphragms sheathed with wood panels were conducted at McGill University (Nikolaidou & Latreille, 2016). Nikolaidou concluded that diaphragms fastened around their full perimeters demonstrate higher strength. In addition, any change in the screw size results in different connection response and failure mode (Nikolaidou & Latreille, 2016).

Seismic response of a full-scale tested ledger-framed building performed by Peterman et al. demonstrated that load resistance of the system is influenced by non-structural and gravity members. In this experimental study, the full-scale building showed high stiffness, low drift, and semi-elastic behavior (Peterman, Asce, et al., 2016). Peterman et al. concluded that deformations at the contact points of the sheathing panels and frame are concentrated within the connectors. (Peterman, Stehman, et al., 2016).

Based on AISI S907 standard, failure modes in diaphragms are either defined as the failure in the connections (screw shear, screw bearing or tearing, screw tilting followed by bearing, pull-over and pull-out of the fasteners) or failure due to the buckling of the diaphragms (out of plane buckling of the deck) (American Iron and Steel Institute (AISI S907), 2017).The Canadian Cold-Formed Steel Research group at University of Waterloo discussed that the dominant failure mode in cold-formed steel shear walls is sheathing failure, initiated at the location of the connections; however, rupture of the sheathing-to-framing connections, sheathing separation from the frame, and failure of the steel studs in the frames sheathed in both sides are probable. Xu and Martinez concluded that sheathing and stud failure are the governing failure modes in the specimens sheathed with OSBs on one side and both sides respectively (Xu & Martínez, 2006).

To validate the results of the experimental tests, numerical models have been created by different researchers. Folz and Filiatrault verified the results of the full-scale wood framed shear walls under cyclic loading via a computational model resulted from a simple numerical formulation for the analysis of the wood-framed shear walls (Bryan Folz & Filiatrault, 2001). Folz and Filiatrault concluded that the non-linear performance of the wood-sheathed shear walls is highly affected by the interaction between fasteners and sheathing boards (Bryan Folz & Filiatrault, 2001).

In a study at Bucknell University, the results of a computational modeling in OpenSees software were compared with the resultant deflections computed based on AISI S213-07, and the response of the experimental tests conducted at University of Northern Texas (Hein Tun, 2014). In this study, the non-linear strength was considerably higher than that of experimental results. The author believes that the interaction among fasteners, sheathing panels and framing elements could be thoroughly captured when all fasteners are modeled (Hein Tun, 2014).

In another research developed by Buonopane et al., the results of the numerical model in OpenSees software showed that reaching to the peak lateral loads did not occur in the same displacement

cycles for the experimental test and computational modeling. Moreover, lateral displacement and energy dissipation of the computational models were lower than those of experimental tests (Buonopane et al., 2015).

Several experimental tests and a finite element modeling were performed at the University of Massachusetts Amherst to evaluate the pull-out capacity of the screw-fastened connections. Castaneda et al. investigated the strength and moment-rotation stiffness of the connections in the specimens sheathed with fiber-cement boards and steel decks. It was concluded that the moment-rotation stiffness and strength of the connections increase considerably with an increase in the thickness of the steel deck, and higher peak strength is achieved with an increase in the number of the fasteners per unit width of the deck (Castaneda & Peterman, 2021).

This study investigates the progression of the failure by a computational model. The results of the numerical study is compared to the results of the recent experimental test conducted at the University of Massachusetts Amherst, and the design calculations recommended by AISI S310 and S100. Diaphragm shear strength, progression of the failure, and system deformation of the computational model are compared with the experimental tests. This research aims to shed light on the load transfer mechanism of the cold-formed steel diaphragms sheathed with steel decks.

2. Cold-Formed Steel Diaphragm Experimental Testing

A 10 ft x 15 ft cold-formed steel diaphragm was tested based on the cantilever testing method in AISI S907 (American Iron and Steel Institute (AISI S907), 2017), to investigate the lateral behavior of the diaphragm sheathed with steel deck. In-plane loads are distributed around the perimeter of the diaphragm owing to the design of the test rig.

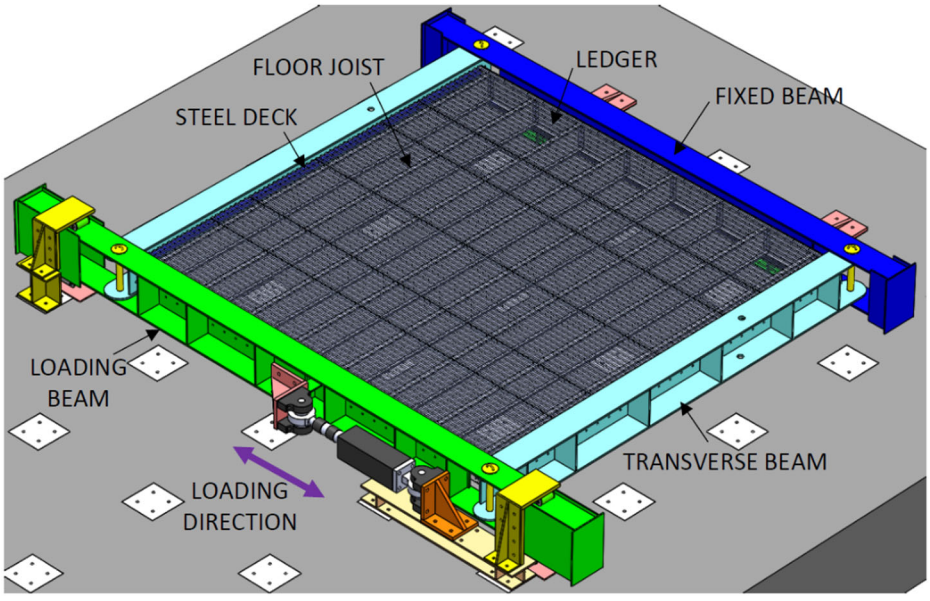

Figure 1: Tested diaphragm fixed in the test rig

2.1 Geometry and Test Setup of the Tested Diaphragm

The experimental test is a 10 ft x 15 ft (4572 mm x 3048 mm) cold-formed steel diaphragm consisting of two identical CFS unlipped channels as the ledgers. Eight studs are attached to the ledgers with even spacing, 2 ft (609.6 mm), as the joists of the system. Joists are connected to the

ledgers via equal-leg clip angles, each of which fastened to the web of the ledger and joist with twelve self-drilling #12 screws in total. Ultimately, the frame is capped with the corrugated steel deck. Figure 1 shows the configuration of the cold-formed steel diaphragm installed in the test rig.

As it is shown in Fig. 1, the rig frame consists of four C-shaped beams. One side of the rig frame is fixed to the floor, simulating the fixed end of a cantilever. The opposite side of the rig is able to move when the load is applied by a hydraulic actuator along the loading direction.

2.2 Test Parameters of the CFS Diaphragm

The CFS diaphragm is assembled with two 12 in (304.8 mm) deep unlipped channels as the ledgers. The width of the flange is 2 in (50.8 mm), and the thickness of the ledger section is 54 mils (1.37 mm). Eight C-shaped joists with 12 in (304.8 mm) depth, 2 in (50.8 mm) flange width and 54 mils (1.37 mm) section thickness are connected to the ledgers via clip angles. The joists are spaced 2 ft (610 mm) apart.

Table 1: Test Matrix of the CFS Diaphragm Components

Element	Dimensions (in)		Design Thickness (in)
Ledger (1200T200-54)	Web Depth	12 (304.8 mm)	0.0566 in (1.37 mm)
	Flange Width	2 (50.8 mm)	
Joist (1200S200-54)	Web Depth	12 (304.8 mm)	0.0566 in (1.37 mm)
	Flange Width	2 (50.8 mm)	
Clip Angle	Legs Width	3.5 (88.9 mm)	0.0566 in (1.37 mm)
	Length	11 (279.4 mm)	
Corrugated Steel Deck	Total Width	35 (889 mm)	0.0239 in (0.60 mm)

Figure 2: Photograph of the CFS diaphragm fixed in the rig before and after the steel deck installation

The web of the joist is attached to the web of the ledger using two 11 in (279.4 mm) long clip angles with 3.5 in (88.9 mm) legs. The legs of the angle are fastened to the web of the ledger and joist with total of twelve self-drilling #12 hex washer head screws (each leg is connected with six fastener). The frame is sheathed with 24 mils (0.60 mm) thick corrugated steel deck. The width of each steel deck is 35 in (889 mm). The test matrix of the tested diaphragm components is presented in Table 1. Figure 2 shows the pictures of the diaphragm fixed in the test rig before and after the installation of the steel deck.

Three various connections are defined to fix the steel deck. Edge connections, self-drilling #12 hex washer head screws, fasten the steel deck to the flange of the ledgers in the edge of the system. Support connections, self-drilling #12 hex washer head screws, connect the steel deck to the flange of the joists of the diaphragm. Side-lap connections, self-drilling #10 hex washer head screws, fasten the steel decks to one another. Location and image of the fasteners fixing steel deck to the CFS frame are shown in Figure 3.

The specimen is tested under displacement-controlled monotonic loading with a constant load rate of 0.01 in/sec.

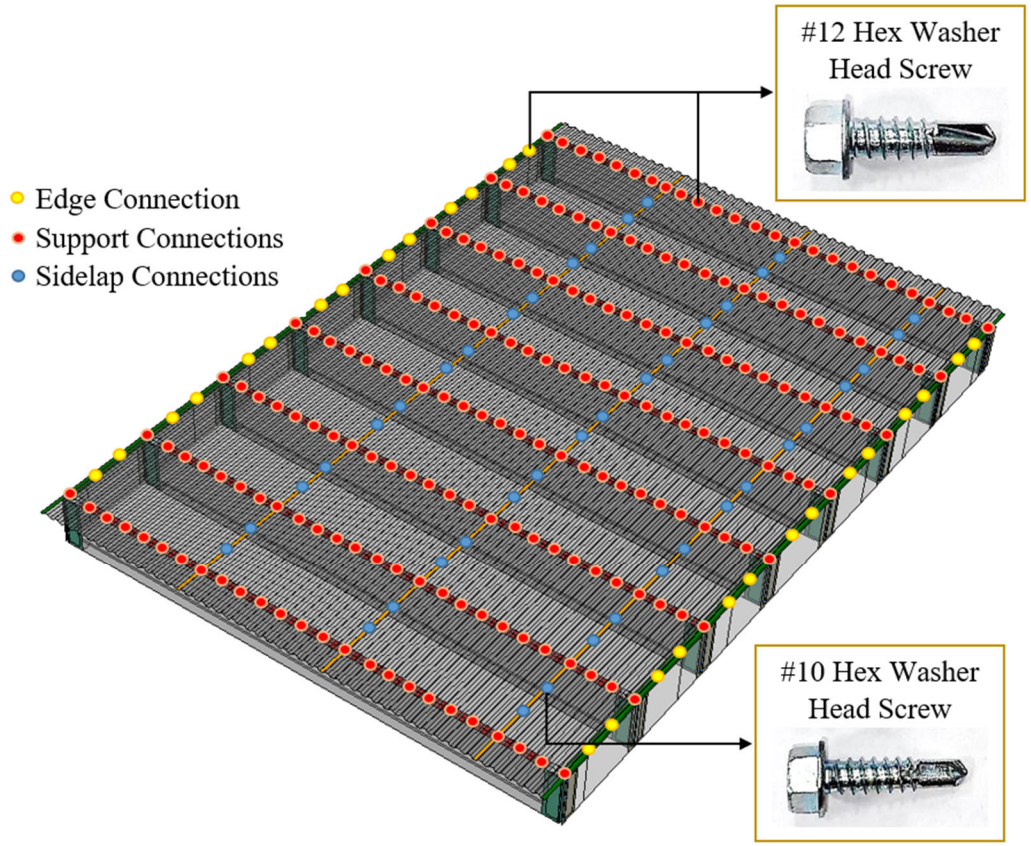

Figure 3: Photograph and Location of the Fasteners Attaching Steel Deck to the CFS Frame

3. Cold-Formed Steel Diaphragm FEM Simulation

The system is modeled as a three-dimensional shell, using ABAQUS software (Dassault System Simulia Corporation, 2014). The model is developed to simulate and capture the lateral response

of the CFS diaphragm sheathed with steel deck under monotonic loading to the extent to which the progression of failure and deformation of the frame can be explored.

3.1 Model Geometry and Material Properties

Ledgers, joists, clip angles and steel deck are modeled based on the geometry and dimensions of the elements in the experimental test. Four-node thin shell (S4R) elements are used to model parts of the computational model. Steel is defined as a homogeneous bi-linear elastic-perfectly-plastic material. Material properties of the elements are summarized in Table 2.

Table 2: Material Properties of the CFS Diaphragm Components

Element	Yield Strength (Fy) (ksi)	Young's Modulus (ksi)	Poisons Ratio
Ledger			
Joist	50 (345 MPa)	29500 (203,500 MPa)	0.3
Clip Angle			
Steel Deck	80 (550 MPa)	29500 (203,500 MPa)	0.3

3.2 Contact Interactions and Connections of the Computational Simulation

The behavior of six contact pairs are defined as surface-to-surface in the contact interactions. Surface-to-surface formulation is used for the surfaces placed parallel to each other. Since both surfaces are deformable, the stiffer one is chosen to be the master surface (Dassault System Simulia Corporation, 2014). Finite sliding is used for the sliding formulation, allowing potential sliding, rotation and separation between the contact surfaces. All six contact pairs are illustrated in Figure 4.

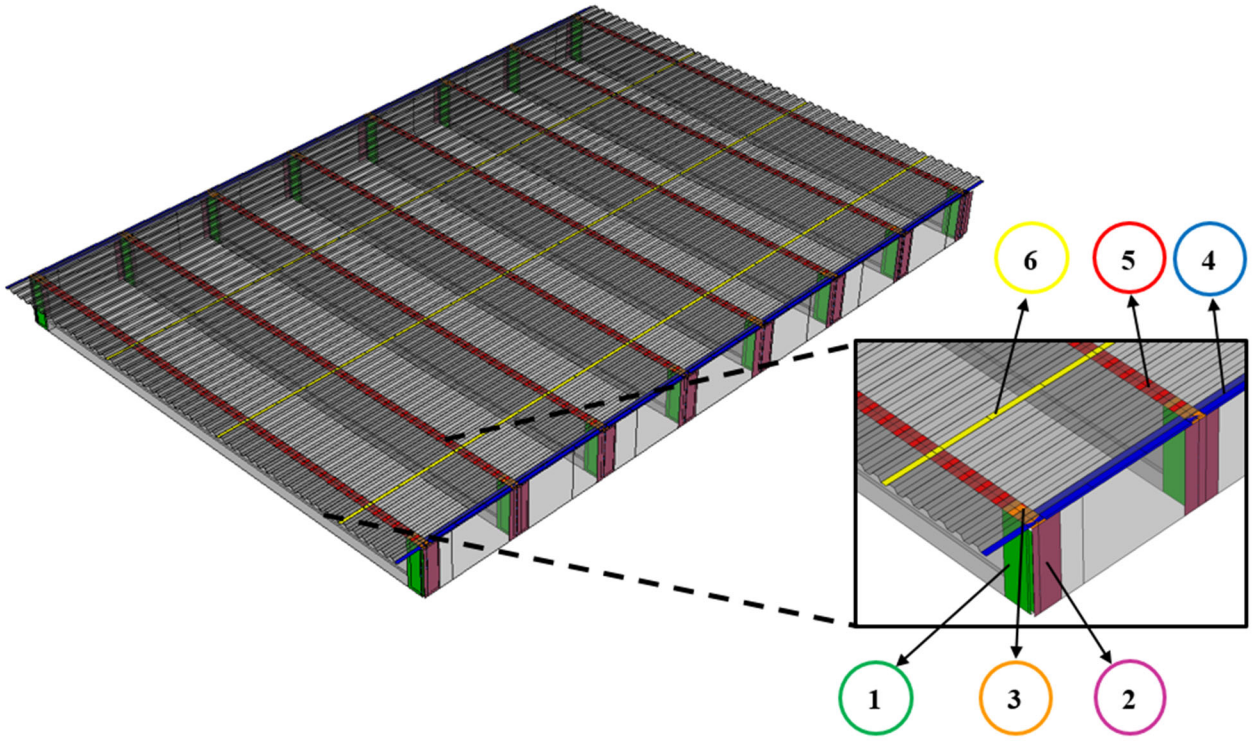

Figure 4: Contact Pairs of the Diaphragm Model: (1) Clip Angle-to-Joist Web – (2) Clip Angle-to-Ledger Web – (3) Ledger Flange-to-Joist Flange – (4) Ledger Flange-to-Steel Deck – (5) Joist Flange-to-Steel Deck – (6) Steel Deck-to-Steel Deck

Two types of contact behavior are defined as normal and tangential for the interaction property of each pair of contacts. Regarding the normal behavior, "Hard" contact is used as the pressure-overclosure interaction, and non-linear behavior is considered for the contact stiffness. Regarding the tangential behavior, a penalty formulation with a friction coefficient equal to 0.2 is considered.

According to the experimental test, six fastened connections are defined in this computational model, three of which are shown in Fig. 4. These connections fastened the corrugated steel deck to the system (a detailed description is presented in section 2.2). Other three connections are depicted in Figure 5.

To simplify the geometry and reduce the analysis time of the model, connections are defined as wires with a multi-linear elastic behavior to simulate fastener shear and pull-out behavior considering local coordinates of the connectors. Shear behavior of the connections are obtained by either interpolation or extrapolation based on the load-displacement characterization of the connections extracted from the experimental work conducted in Virginia Polytechnic Institute and State University, (Pham & Moen, 2015; Tao & Moen, 2017). Pull-out behavior of the connections are defined as a rigid behavior due to the absence of data for the aforementioned connections.

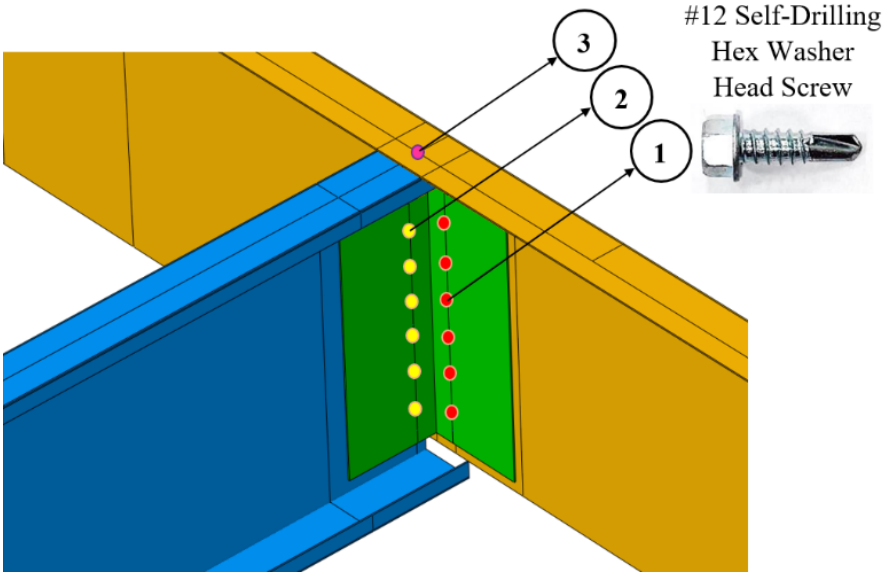

Figure 5: Fastened Connections: (1) Ledger Web-to-Clip Angle – (2) Joist Web-to-Clip Angle – (3) Ledger Flange-to-Joist Flange

3.3 Meshing of the Computational Model

Elements in the diaphragm simulation are modeled as the 4-node thin shell elements (S4R). An approximate aspect ratio of 1:1 is used to structure a quadrilateral mesh. A coarser mesh, 12 mm, is defined for those part of the elements where connections are non-existent. A finer mesh, 6 mm, is used for the regions in close proximity to the connections.

3.4 Boundary Conditions and Loading of the Simulation

Boundary conditions and loading are depicted in Figure 6.

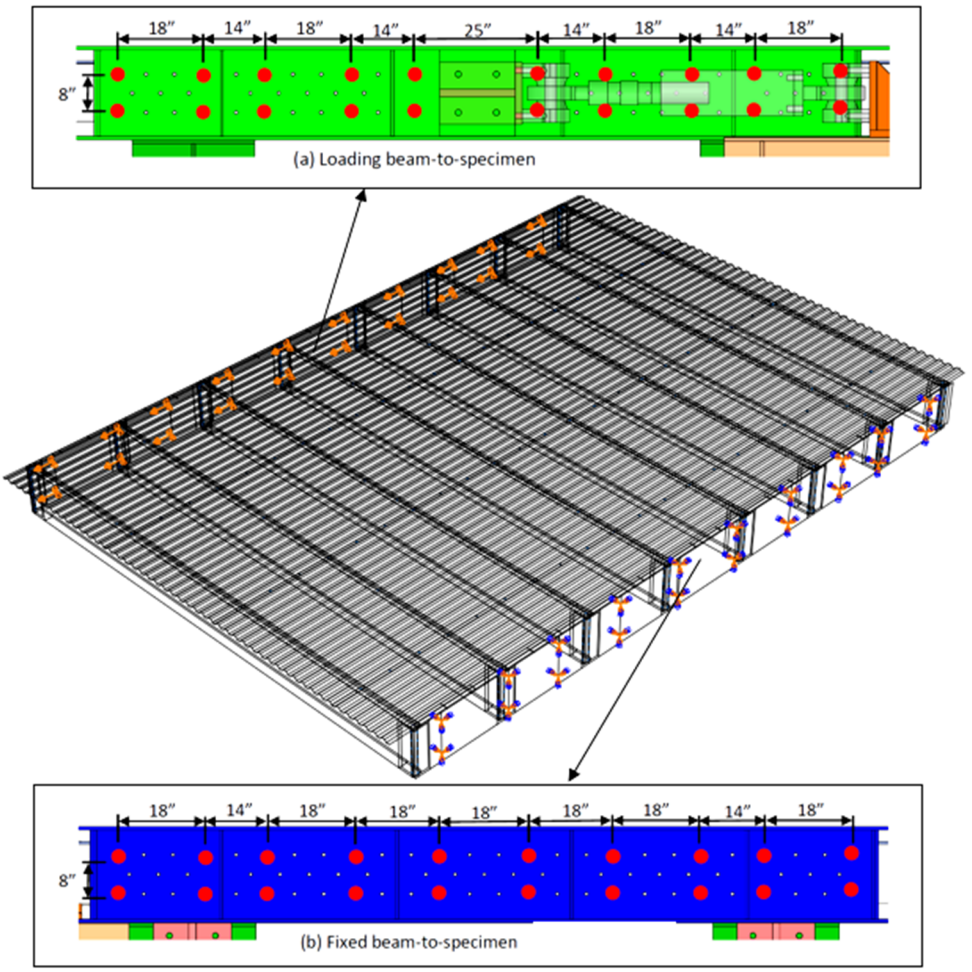

Figure 6: Boundary Conditions and Loading in the Simulated Diaphragm: (a) Loading Points on the Rig Frame – (b) Fixed Points on the Rig Frame

One side of the frame is fixed, and the load is applied as a ramp function to the other side of the diaphragm. The loaded and fixed points of the experimental test are illustrated in Fig 6.a and 6.b respectively. The same points are also modeled on the ledgers of the computational simulation.

4. Equation Calculations Based on the Code

Shear strength of the screws (P_{nv}) are calculated based on the Equations (1), (2), (3) or (4), (5) (American Iron and Steel Institute (AISI S100), 2016).

For $t_2/t_1 \leq 1.0$, P_{nv} is considered as the minimum of:

$$P_{nv} = 4.2\,(t_2^3 d)^{1/2}\,F_{u_2} \tag{1}$$

$$P_{nv} = 2.7\;\;t_1\,d\,F_{u_1} \tag{2}$$

$$P_{nv} = 2.7\;\;t_2\,d\,F_{u_2} \tag{3}$$

For $t_2/t_1 \geq 2.5$, P_{nv} is considered as the minimum of:

$$P_{nv} = 2.7\ t_1\ d\ F_{u_1} \tag{4}$$

$$P_{nv} = 2.7\ t_2\ d\ F_{u_2} \tag{5}$$

For $1.0 \leq t_2/t_1 \leq 2.5$, P_{nv} is obtained by linear interpolation between the two cases mentioned previously (American Iron and Steel Institute (AISI S100), 2016).

Where P_{nv} is the nominal shear strength of the screw, t_1 is the thickness of the element in contact with the screw head, t_2 is the thickness of the element not in contact with screw head, d is the nominal diameter of the screw, F_{u_1} is the tensile strength of the element in contact with the screw head and F_{u_2} is the tensile strength of the element not in contact with the screw head (American Iron and Steel Institute (AISI S100), 2016). Table 3 summarizes the variables used in the Eq. 1, 2, 3, 4 and 5.

Table 3: Summarized Variables Used for Nominal Shear Strength Calculations

Connection Name	Connection Type	t1 (in)	t2 (in)	F_{u1}(ksi)	F_{u2} (ksi)	d (in)	Pnv (kips)
24 mils – to - 54 mils - #12 (Steel Deck-to-Ledger/Joist)	Edge and Support Connections	0.0239 (0.60 mm)	0.0566 (1.43 mm)	90 (615 MPa)	65 (450 MPa)	0.216 (5.48 mm)	1.25 (5.56 kN)
24 mils – to - 24 mils - #10 (Steel Deck-to-Steel Deck)	Sidelap Connections	0.0239 (0.60 mm)	0.0239 (0.60 mm)	90 (615 MPa)	90 (615 MPa)	0.190 (4.82 mm)	0.61 (2.71 kN)

Distribution of the reaction forces at every sheathing connection of a steel deck is considered to calculate the diaphragm shear strength. Nominal shear strength per unit length of a diaphragm is governed by the strength of the connections, S_{nf}. Connection strength is considered as the minimum of the three limit states, S_{ni}, S_{nc}, and S_{ne}, defined as follows (American Iron and Steel Institute (AISI S310), 2016):

S_{ni} = Nominal shear strength per unit length of diaphragm governed by connections at interior panels or edge panels

S_{nc} = Nominal shear strength per unit length of diaphragm governed by support connections at the corners of interior panels or edge panels

S_{ne} = Nominal shear strength per unit length of diaphragm governed by connections along the edge parallel to the panel span in the edge panel at the diaphragm reaction line

$$S_{nf} = Min\,\{S_{ni}, S_{nc}, S_{ne}\} = Min\,\{1.99, 1.67, 3.07\} = 1.67\ {}^{kips}/_{ft} \tag{6}$$

The calculations of S_{ni}, S_{nc}, and S_{ne}, represented in detail in Appendix A (Castaneda, 2022), result in the nominal shear strength per unit length of the diaphragm being equal to 1.67 kips/ft (Eq. (6)).

5. Results of the Diaphragm Floor Sheathed with Steel Deck

5.1 Lateral Response of the CFS Diaphragm Sheathed with Steel Deck

The shear results of the calculations based on AISI S310 and S100, (American Iron and Steel Institute (AISI S100), 2016; American Iron and Steel Institute (AISI S310), 2016), experimental test and computational model are compared to evaluate the shear response of the Diaphragm. Figure 7.A illustrates the shear strength of the diaphragm vs. displacement of the experimental model, computational simulation, and calculations based on AISI S310. The Von-Mises stress of the CFS diaphragm is shown in Fig. 7.B.

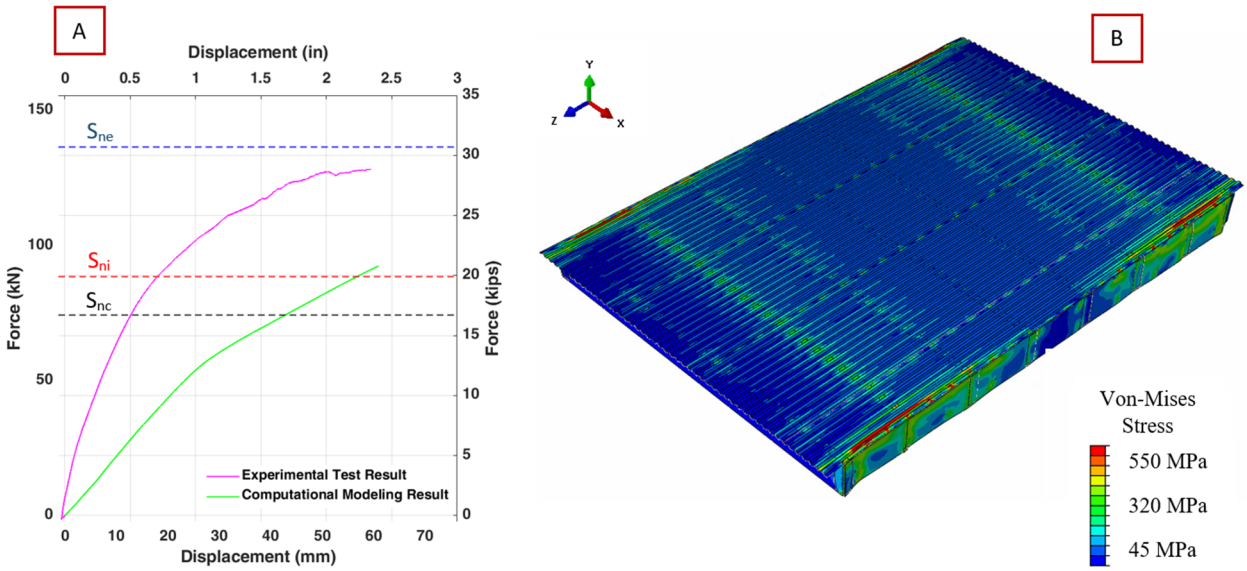

Figure 7: Lateral Response of the Diaphragm: (A) Shear Strength of the CFS Diaphragm (Force-Displacement Curve) – (B) Von-Mises Stress in the Computational Model

As it is shown in Fig. 7.A, the shear strength of the computational analysis is lower than the results of the experimental test, and higher than the estimated shear strength recommended by AISI S310. It is worth noting that the shear strength of the computational model is highly dependent on the definition of the connections behavior. Therefore, the accuracy of the simulation results increases significantly by using the exact multi-linear responses of the screw-fastened connections in place of the interpolated or extrapolated ones.

5.2 Progression of Failure in the CFS Diaphragm Sheathed with Steel Deck

It was observed in the experimental test that the tilting of the side-lap screws occurred as the initial damage, followed by bearing in the support connections at the intersection of the side-lap and support connections (Figure 8.A). Increased damage in the side-lap connections leads to more relative displacement between the sheathing panels, transferring further load to the support connections. This causes the damage to be propagated from the side-lap screws toward the center line of the steel decks (Figure 8.B). With damage propagation in the vicinity of the side-lap connections, bearing in the edge connections increases severely. The same load path and progression of failure are clearly recognizable in the computational simulation (Fig. 8 and 9). As it is shown in the finite element model in Fig. 8 and 9, the load is transferred from the steel deck to the side-lap connections, causing initial damage to these connections. Subsequently, damage of the support connections is occurred at the location of the side-lap intersection. Ultimately, the damage is propagated to the edge connections due to the increase in the applying load.

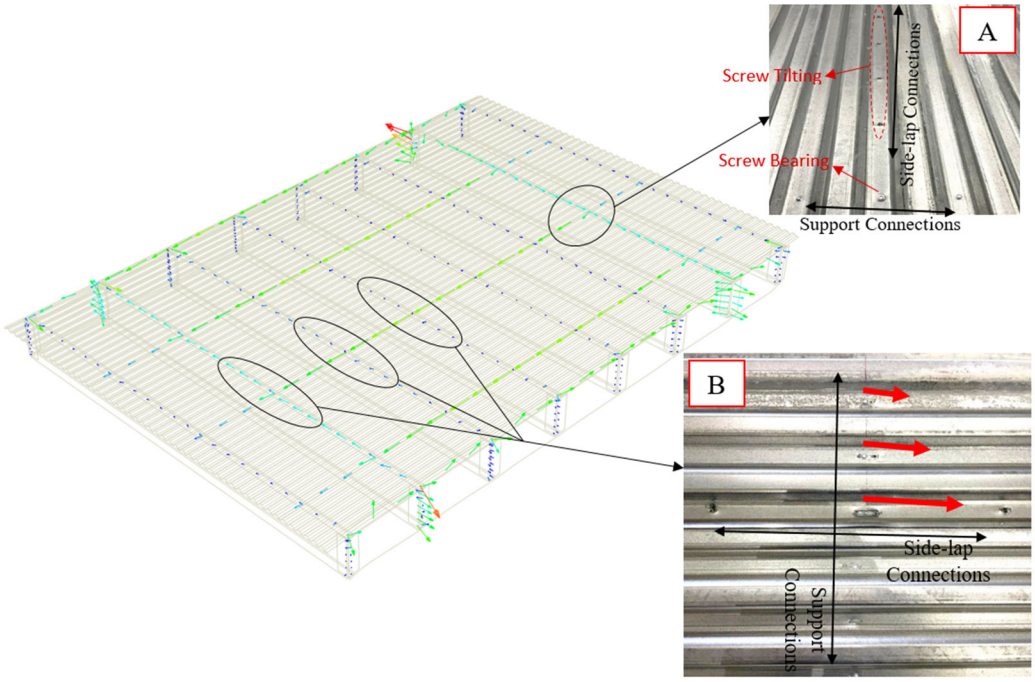

Figure 8: Propagation of Damage during Loading: (A) Initial Damage: Screw Tilting and Bearing – (B) Propagation of Damage

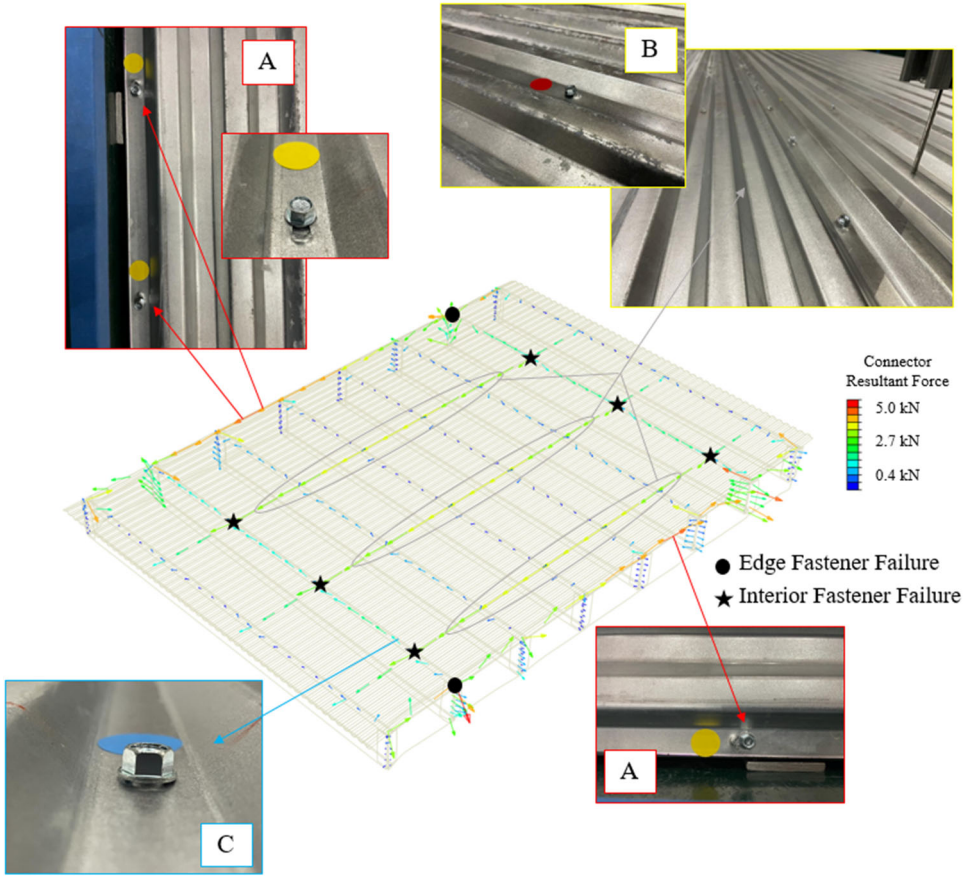

Figure 9: Failure: (A) Edge Connections, Bearing, Flush Head – (B) Side-lap Connections, Screw Tilting, No Flush Head – (C) Support Connections, Incipient Tilting/Bearing, Tilted Head

As it is illustrated in Fig. 9, the edge connections damaged considerably due to the bearing (Fig. 9.A), the side-lap connections damaged by tilting of the screws (Fig. 9.B), and the support fasteners tilted slightly (Fig. 9.C) in the experimental test. These damages are also recognizable in the computational model by the magnitude of the connection loads (Fig. 9). Six connection failures at the end of the computational analysis are identified as it is shown in Fig. 9; two of which are the edge connection failures, and the others are the connection failures at the intersection of the side-lap and support fasteners. As it is presented in Section 4 of this paper, the shear strength, according to AISI S310, is governed by the failure of the corner fasteners at interior or edge panels (S_{nc}). The same failure is observed after the tilting of the side-lap connections in both of the experimental and computational models.

5.3 Observed Deformation in the CFS Diaphragm Sheathed with Steel Deck

It was recognized in the experimental test that the load was transferred from the steel deck to the side-lap connections, and then to the edge and support connections. With damage in the deck fasteners, the transmitted load to the joists of the frame causes flexural torsion in the joists. This deformation of the joists results in the buckling of the clip angles on one side of the frame and creation of a gap between upper part of the clip angle and the joist web on the other side. These two types of deformation are illustrated in Figure 10. The same load path in the finite element model leads to the same resultant deformation in the connections of the frame. The buckling of the clip angle and the gap between the upper part of the clip angle and joist web are recognizable in the experimental and computational tests in Fig. 10.A and 10.B respectively.

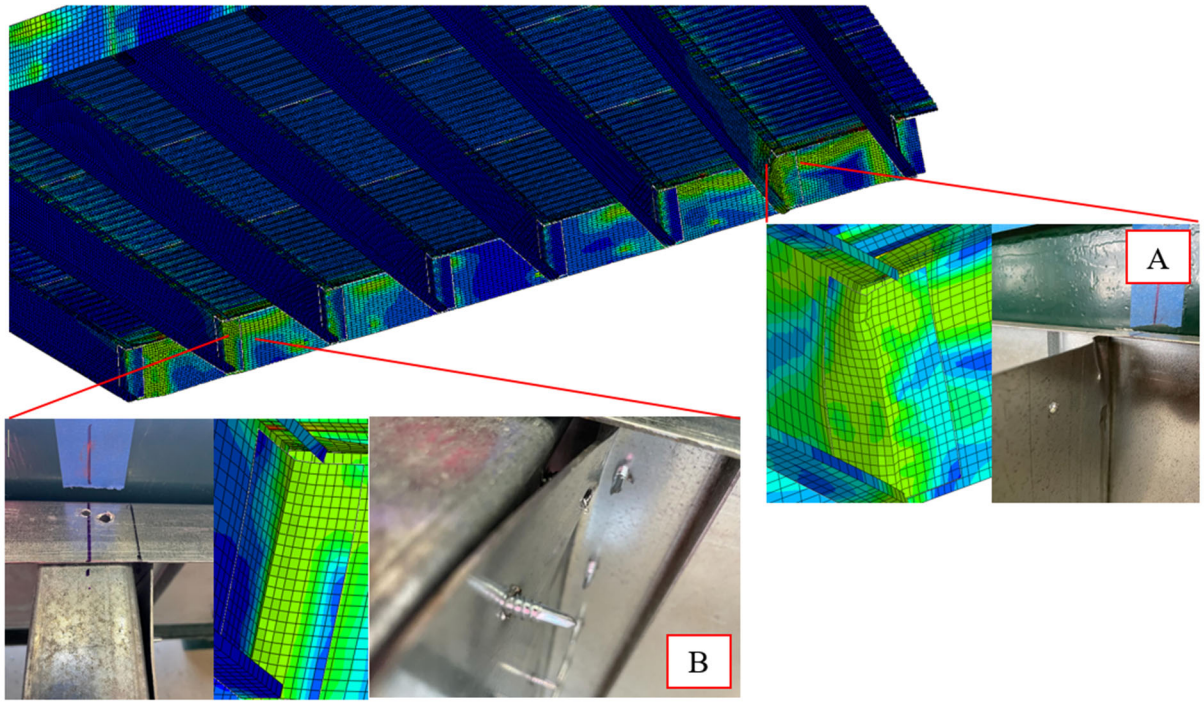

Figure 10: Observed Deformation: (A) Buckling of the Clip Angle – (B) Gap between the Clip Angle and Joist Web

6. Conclusions

In this study, a three-dimensional shell model of a CFS diaphragm sheathed with steel deck is created and developed to capture the progression of the failure in the connections under monotonic

loading. The results of the finite element model is compared with the response of the CFS diaphragm tested experimentally at the University of Massachusetts Amherst. The shear strength of the system is higher than the shear strength calculated based on AISI S300 and lower than the shear strength achieved by the experimental test. The experimental and computational models show the same progression of failure. The load is transferred from the steel deck to the side-lap fasteners, then support and edge connections. Therefore, the damage of the connections is initiated in the side-lap screws, propagating to the support connections located at the intersections of the side-lap connections. Finally, the edge connections experience significant damage due to the higher load transfer from the side-lap screws. Load transfer from the steel deck to the frame causes flexural torsion in some joists of the model, leading to the buckling of the clip angle on one side of the frame and creation of a gap between the upper part of the clip angle and joist web on the other side of the diaphragm.

Acknowledgments

The authors would like to thank Canam Steel, Super Stud and ClarkDietrich Corporations for their in-kind support through the donation of the specimen materials. The assistance and guidance provided by the lab technician at UMass Amherst, Mr. Mark Gauthier, is highly appreciated.

References

American Iron and Steel Institute (AISI S100). (2016). North American standard for the design of cold-formed steel structural members.

American Iron and Steel Institute (AISI S310). (2016). North American standard for the design of profiled steel diaphragm panels.

American Iron and Steel Institute (AISI S907). (2017). Test standard for determining the strength and stiffness of cold-formed steel diaphragms by the cantilever test method.

Bryan Folz, B., & Filiatrault, A. (2001). CYCLIC ANALYSIS OF WOOD SHEAR WALLS. Em JOURNAL OF STRUCTURAL ENGINEERING.

Buonopane, S. G., Bian, G., Tun, T. H., & Schafer, B. W. (2015). Computationally efficient fastener-based models of cold-formed steel shear walls with wood sheathing. Journal of Constructional Steel Research, 110, 137–148. https://doi.org/10.1016/j.jcsr.2015.03.008

Castaneda, H. (2022). LATERAL RESPONSE OF COLD-FORMED STEEL DIAPHRAGMS LATERAL RESPONSE OF COLD-FORMED STEEL DIAPHRAGMS WITH VARIABLE SHEATHING WITH VARIABLE SHEATHING. https://doi.org/10.7275/31023083

Castaneda, H., & Peterman, K. D. (2021). Moment-rotation response of cold-formed steel joist-to-ledger connections with variable-finishes in ledger-framed construction. Journal of Constructional Steel Research, 176. https://doi.org/10.1016/j.jcsr.2020.106396

Dassault System Simulia Corporation. (2014). ABAQUS/CAE Documentation, Version 6.14-4. www.simulia.com.

Hein Tun, T. (2014). Fastener-Based Computational Models of Cold-Formed Steel Shear Walls. https://digitalcommons.bucknell.edu/honors_theses/249

Nikolaidou, V., & Latreille, P. (2016). Characterization of CFS Framed Diaphragm Behaviour American Iron and Steel Institute.

Peterman, K. D., Asce, A. M., Matthew, Stehman, J. J., Madsen, R. L., Asce, M., Buonopane, S. G., Nakata, N., & Schafer, B. W. (2016). Experimental Seismic Response of a Full-Scale Cold-Formed Steel-Framed Building. I: System-Level Response.

Peterman, K. D., Stehman, M. J. J., Madsen, R. L., Buonopane, S. G., Nakata, N., & Schafer, B. W. (2016). Experimental Seismic Response of a Full-Scale Cold-Formed Steel-Framed Building. II: Subsystem-Level Response. Journal of Structural Engineering, 142(12). https://doi.org/10.1061/(asce)st.1943-541x.0001578

Pham, H. S., & Moen, C. D. (2015). STIFFNESS AND STRENGTH OF SINGLE SHEAR COLD-FORMED STEEL SCREW-FASTENED CONNECTIONS.

Schafer, B. W., Li, Z., & Moen, C. D. (2010). Computational modeling of cold-formed steel. Thin-Walled Structures, 48(10–11), 752–762. https://doi.org/10.1016/j.tws.2010.04.008

Tao, F., & Moen, C. (2017). RP17-2, Monotonic and Cyclic Response of Single Shear Cold-Formed Steel-to-Steel and Sheathing-to-Steel Connections Monotonic and Cyclic Response of Single Shear Cold-Formed Steel-to-Steel and Sheathing-to-Steel Connections.

Xu, L., & Martínez, J. (2006). Strength and stiffness determination of shear wall panels in cold-formed steel framing. Thin-Walled Structures, 44(10), 1084–1095. https://doi.org/10.1016/j.tws.2006.10.002

Zhang, S., & Xu, L. (2018). Determination of equivalent rigidities of cold-formed steel floor systems for vibration analysis, Part I: Theory. Thin-Walled Structures, 132, 25–35. https://doi.org/10.1016/j.tws.2018.08.001